



## Tunable Fabry–Pérot filter based on one-dimensional photonic crystals with liquid crystal components

J. Cos, J. Ferre-Borrull, J. Pallares, L.F. Marsal\*

*Nanoelectronic and Photonic Systems, Departament d'Enginyeria Electrònica, Elèctrica i Automàtica, Universitat Rovira i Virgili, Avda. Països Catalans 26, 43007 Tarragona, Spain*

### ARTICLE INFO

#### Article history:

Received 17 August 2008

Received in revised form 24 October 2008

Accepted 26 November 2008

#### Keywords:

Liquid crystal

Photonic crystal

Fabry–Pérot

Transfer matrix method

Anisotropic materials

### ABSTRACT

A theoretical study of a tunable Fabry–Pérot multilayer structure composed of alternating layers of silicon and liquid crystal is presented and analyzed. The structure possesses two resonant frequencies within the stop band with tunable wavelengths and transmission properties. Tuning is achieved by allowing different orientations of the liquid crystal optical axes within the cavity and within the mirrors, while keeping the optical axes parallel to the layers. Applying the transfer matrix method for thin layers of anisotropic materials we demonstrate that the resonant wavelengths depend on the difference between the liquid crystal optical axis orientations. Besides, we are able to obtain a complete characterization of the structure in the form of its Jones matrix. From this, we propose an optical two-channel equalizer for applications around 1.55  $\mu\text{m}$  that allows tuning the two resonant wavelengths and their relative amplitude levels.

© 2008 Elsevier B.V. All rights reserved.

### 1. Introduction

Photonic crystals (PCs) are periodic dielectric or metal-dielectric synthetic structures designed to influence the propagation of electromagnetic waves in the same way as the periodic potential in semiconductor crystals influences the electron motion by defining allowed and forbidden energy bands. Since first proposed [1,2] their potential scientific and technological applications have inspired great interest among researchers. Photonic crystals offer a significant opportunity to create new optical devices and hold a great potential for many significant applications, such as lasers and solar cells [3], high quality resonators and filters [4], optical fibers [5], etc.

In the last decade many efforts have been spent towards tuning the properties of photonic crystals in order to design switchable or dynamical devices. Several structures combining photonic crystals with nonlinear optical (NLO) materials or liquid crystal (LC) materials have been proposed [6–9]. In the former case, a high-intensity control signal with frequency outside the bandgap changes the properties of the crystal [10]. In the case of LC's, their refractive index can be varied either by changing the operating conditions (i.e. temperature) or applying an external electric field [11].

Particularly, one-dimensional photonic crystals are known for several decades [12,13] in the form of periodic multilayer coatings, consisting of stacked pairs of alternate dielectric or metal-dielectric layers with a large contrast of the dielectric constant along

the propagation direction. Tuning the properties of such structures can be achieved by the infiltration of several layers with LC, as has been proposed by several authors. In particular, Alagappan et al. [14] propose alternating anisotropic (E7 LC) and isotropic (silicon) layers and study the bandgap for each polarization. Others authors as Mandatori et al. [15] or Vandenberg et al. [16] propose photonic crystals that alternate two anisotropic layers with alternate orientation of the optical axes, and they discuss the polarization dependence of the transmission. Ha et al. [17] present the electrical control of the director angle of LC layers alternated with isotropic layers. Finally, Liu et al. [18] proposed a Mach-Zehnder interferometer in which the phase of light propagation at the two arms can be varied by means of a section in each arm infiltrated with LC, whose optical axes can be varied independently.

A particular case of one-dimensional multilayer structures are the Fabry–Pérot (FP) interferometers, that can be seen as a one-dimensional photonic crystal with a defect that acts as a resonant cavity. Tuning the resonant properties of such structures by the introduction of LC in the defect layer has been reported in the literature. Hirabayashi et al. [19] study the application of a tunable FP structure with LC defect for wavelength-division multiplexing (WDM). Ozaki et al. [20] propose this structure to the design and fabrication of tunable lasers. They pay special attention to the estimation of response time for the defect mode switching. In all these works the LC optical axis is varied from an alignment parallel to the layers to a perpendicular alignment.

Studies on the actual practical implementation of the electric field control of the LC optical axis director have also been published: Zografopoulos et al. [21] study the orientation of the LC

\* Corresponding author. Tel.: +34 97 755 9625; fax: +34 97 755 9605.  
E-mail address: [lluis.marsal@urv.cat](mailto:lluis.marsal@urv.cat) (L.F. Marsal).

directors in a one-dimensional photonic crystal slab applying voltage by means of a ITO layer above the slab; Tolmachev et al. [22] fabricate tunable photonic one-dimensional structures based on alternate layers of LC and silicon.

In this paper we link the previously stated facts: (i) FP tunable structures are of particular interest because of their possible applications, and (ii) independent variation of the LC optical axis at different points of the photonic structure provides the structure with additional features, to propose a tunable FP structure where the LC optical axis can be varied independently at the mirrors and at the cavity. In contrast to previous studies tunability is achieved while maintaining the LC optical axes parallel to the layers.

The rest of this paper is organized as follows: Section 2 is an overview of the numerical method employed to obtain the transmission Jones matrix of the structure. In Section 3 we analyze the transmission properties of the structure as a function of the LC optical axes orientation at the mirrors and at the cavity. In particular, we will show that allowing different optical axis orientations at the FP mirrors and at the cavity allows the tuning of the resonant frequencies and of the transmittance at each resonant wavelength. Finally, in Section 4 we propose a tunable two-channel optical equalizer based on the tunable FP structure and two polarizers and we analyze and discuss its performance for different relative orientations between the LC optical axes at the mirrors and at the cavity and the polarizers.

## 2. Jones matrix of a multilayer structure with anisotropic components

We propose a Fabry–Pérot multilayer structure composed of two one-dimensional photonic crystals, acting as mirrors, surrounding a resonant cavity, where the materials composing the layers and the cavity can be anisotropic. Fig. 1 shows a schematic view of the structure. The modeling of a multilayer structure with anisotropic components is well studied in several references [23,24]. Here we only aim at giving an overview of the method we have used: the  $4 \times 4$  transfer matrix method introduced by Yeh [24]. This method is based on two kinds of  $4 \times 4$  matrixes, the dynamical matrix  $D$  (related with the interfaces) and the propagation matrix  $P$  (related with the propagation along the layers). In order to simplify equations, we consider normal incidence in this paper. We define the  $z$ -axis as normal to the layers. With this, the electric fields are represented as 4-vectors where the components correspond to the complex amplitude of the waves propagat-

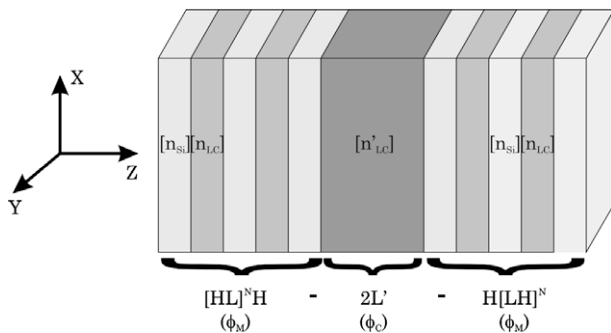


**Fig. 1.** Schematic view of the Fabry–Pérot structure composed of two mirrors with  $N + 1$  quarter-wave (optical thickness) layers of silicon and  $N$  quarter-wave layers of Liquid Crystal separated by a half-wave layer of liquid crystal as cavity. The  $\phi_M$  and  $\phi_C$  indicate the angle of the LC optical axis with the  $y$  axis, taking into account that the LC optical axis is parallel to the layers. The prima superscript for the cavity indicates that the angles  $\phi_M$  and  $\phi_C$  can be different. The optical thicknesses are calculated taking the refraction index of the LC in the isotropic state.

ing in the positive and negative direction of the  $z$ -axis and polarized along the two main polarization directions, which will be labeled with the  $x$  and  $y$  direction.

The dynamic and propagation matrixes are defined for each layer of the structure. Their explicit expression is:

$$D(j) = \begin{pmatrix} e_x \cdot \mathbf{p}_1^{(j)} & e_x \cdot \mathbf{p}_2^{(j)} & e_x \cdot \mathbf{p}_3^{(j)} & e_x \cdot \mathbf{p}_4^{(j)} \\ e_y \cdot \mathbf{q}_1^{(j)} & e_y \cdot \mathbf{q}_2^{(j)} & e_y \cdot \mathbf{q}_3^{(j)} & e_y \cdot \mathbf{q}_4^{(j)} \\ e_y \cdot \mathbf{p}_1^{(j)} & e_y \cdot \mathbf{p}_2^{(j)} & e_y \cdot \mathbf{p}_3^{(j)} & e_y \cdot \mathbf{p}_4^{(j)} \\ e_x \cdot \mathbf{q}_1^{(j)} & e_x \cdot \mathbf{q}_2^{(j)} & e_x \cdot \mathbf{q}_3^{(j)} & e_x \cdot \mathbf{q}_4^{(j)} \end{pmatrix}, \quad (1)$$

$$P(j) = \begin{pmatrix} e^{-i\gamma_1^{(j)}d_j} & 0 & 0 & 0 \\ 0 & e^{-i\gamma_2^{(j)}d_j} & 0 & 0 \\ 0 & 0 & e^{-i\gamma_3^{(j)}d_j} & 0 \\ 0 & 0 & 0 & e^{-i\gamma_4^{(j)}d_j} \end{pmatrix}, \quad (2)$$

where the  $j$  is the layer index, the  $e_x$  and  $e_y$  are the unit vectors in the  $x$  and  $y$  directions, and  $\mathbf{p}_\sigma$  and  $\mathbf{q}_\sigma$  are vectors defined as:

$$\mathbf{p}_\sigma = N_\sigma \begin{pmatrix} \left(\frac{\omega}{c}\right)^2 \varepsilon_{zz} \left[ \left(\frac{\omega}{c}\right)^2 \varepsilon_{yy} - \gamma_\sigma^2 \right] - \left(\frac{\omega}{c}\right)^4 \varepsilon_{yz}^2 \\ \left(\frac{\omega}{c}\right)^4 \varepsilon_{yz} \varepsilon_{xz} - \left(\frac{\omega}{c}\right)^4 \varepsilon_{xy} \varepsilon_{zz} \\ \left(\frac{\omega}{c}\right)^4 \varepsilon_{xy} \varepsilon_{yz} - \left(\frac{\omega}{c}\right)^2 \varepsilon_{xz} \left[ \left(\frac{\omega}{c}\right)^2 \varepsilon_{yy} - \gamma_\sigma^2 \right] \end{pmatrix}, \quad (3)$$

$$\mathbf{q}_\sigma^{(j)} = \frac{\gamma_\sigma}{\mu_0 \omega} e_z \times \mathbf{p}_\sigma^{(j)}, \quad (4)$$

with  $\sigma = 1, 2, 3, 4$ . In Eqs. (3) and (4),  $\varepsilon_{\alpha\beta}$  (with  $\alpha, \beta = x, y, z$ ) are the components of the dielectric tensor for the considered layer,  $\omega$  is the angular frequency of the light,  $c$  is the light speed in vacuum,  $N_\sigma$  are normalization constants such that  $\mathbf{p}_\sigma \cdot \mathbf{p}_\sigma = 1$  and the  $\gamma_\sigma$  are the propagation constants, which can be obtained from the equation:

$$\begin{vmatrix} \left(\frac{\omega}{c}\right)^2 \varepsilon_{xx} - \gamma^2 & \left(\frac{\omega}{c}\right)^2 \varepsilon_{xy} & \left(\frac{\omega}{c}\right)^2 \varepsilon_{xz} \\ \left(\frac{\omega}{c}\right)^2 \varepsilon_{yx} & \left(\frac{\omega}{c}\right)^2 \varepsilon_{yy} - \gamma^2 & \left(\frac{\omega}{c}\right)^2 \varepsilon_{yz} \\ \left(\frac{\omega}{c}\right)^2 \varepsilon_{zx} & \left(\frac{\omega}{c}\right)^2 \varepsilon_{zy} & \left(\frac{\omega}{c}\right)^2 \varepsilon_{zz} \end{vmatrix} = 0. \quad (5)$$

With these definitions, the  $T$  matrix corresponding to the total transfer matrix of a structure composed of  $N$  layers is:

$$T = D^{-1}(\text{air}) \prod_{i=1}^{i=N} (D(i) \cdot P(i) \cdot D^{-1}(i)) \cdot D(\text{air}). \quad (6)$$

Due to the use of anisotropic materials, there can be coupling between the different polarizations both in reflection and in transmission. Therefore we will use the Jones matrix formalism [24,25] since it permits to model this coupling. In this formalism, our structure is represented by a Jones matrix:

$$J = \begin{pmatrix} t_{xx} & t_{xy} \\ t_{yx} & t_{yy} \end{pmatrix}, \quad (7)$$

where  $t_{ab}$  is the Jones transmission coefficient for incoming light polarized in the direction  $b$  and outgoing light polarized in the direction  $a$ . These coefficients are related to the  $T$  matrix of the Eq. (6) through the expressions [24]:

$$t_{xx} = \frac{T(3, 3)}{T(1, 1)T(3, 3) - T(1, 3)T(3, 1)} - \frac{T(3, 1)}{T(1, 1)T(3, 3) - T(1, 3)T(3, 1)}, \quad (8a)$$

$$t_{xy} = \frac{-T(1, 3)}{T(1, 1)T(3, 3) - T(1, 3)T(3, 1)}, \quad (8b)$$

$$t_{yx} = \frac{-T(1, 3)}{T(1, 1)T(3, 3) - T(1, 3)T(3, 1)}, \quad (8c)$$

$$t_{yy} = \frac{T(1, 1)}{T(1, 1)T(3, 3) - T(1, 3)T(3, 1)}. \quad (8d)$$

### 3. Tunable Fabry–Pérot filter with independent liquid crystal optical axis orientation at the mirrors and at the cavity

The structure we propose is a multilayer Fabry–Pérot structure composed of two mirrors surrounding a cavity (see Fig. 1). The mirrors are composed of a periodic stacking of bilayers, with the high index layer made of silicon and the low index layer of liquid crystal, while the cavity is made of LC. The tunability of the filter is achieved allowing the orientations of the LC optical axes at the mirrors and at the cavity to be different. An additional silicon layer must be added to the mirrors to surround the LC cavity and thus to provide mechanical stability to the structure. This additional silicon layer also increases the reflectance maximum value [26]. We have chosen silicon as isotropic material because of its high refractive index at wavelengths with interest in optical communications and because it is compatible with most of the existing fabrication technologies. It is well known that silicon is actually not an isotropic material, however we have considered it as isotropic because the anisotropy is anyway small and to keep the study of the structure simpler. As anisotropic material we have considered the E7 LC, since its director angle can be varied with an applied electric field.

We have chosen the dimensions of the FP structure so that, when the LC is in its isotropic state, the mirrors are composed of quarter-wave layers of silicon and LC, while the cavity is a half-wave layer of LC, for a wavelength of 1.55  $\mu\text{m}$ . Thus, the design can be expressed as  $[\text{HL}]^3\text{H}-2\text{L}'-\text{H}[\text{LH}]^3$  (see Fig. 1), where H stands for a quarter-wave layer of the high refractive index material, and L for a quarter-wave layer of the low refractive index material (the LC). The prima superscript for the cavity indicates that the LC optical axis direction of the cavity can be different to that of the mirrors. We have considered  $n_{\text{si}} = 3.4$  as refractive index of silicon and  $n_o = 1.522$  and  $n_e = 1.704$  as ordinary and extraordinary indexes of E7 LC. The optical axis of the LC in all the layers is kept parallel to the  $xy$  plane.

In contrast with previous works with tunable FP filters, we propose to tune the filter properties by rotating the LC optical axis in the  $xy$  plane. With this configuration we have two degrees of freedom: the angle of the optical axis of the LC within the mirrors,  $\phi_M$ , and the angle of the optical axis of the LC within the cavity,  $\phi_C$ . It must be mentioned that both  $\phi_M$  and  $\phi_C$  are measured with respect to the  $y$  axis. Fig. 2 shows the transmission spectra of the structure for the isotropic state of the LC (Fig. 2a) and for the anisotropic state with angles  $\phi_M = 15^\circ$  and  $\phi_C = 45^\circ$  (Fig. 2b and c). In the isotropic state the transmittance is polarization-independent, while for the anisotropic state the transmittance spectra  $|t_{xx}|^2$  and  $|t_{yy}|^2$  (from the structure Jones matrix) are shown. These figures show that the single resonance present in the isotropic state (at wavelength  $\lambda = 1.55 \mu\text{m}$ ) splits in two resonances,  $\lambda_1 = 1.516 \mu\text{m}$  and  $\lambda_2 = 1.625 \mu\text{m}$ . As it can be observed, the transmittance at each of the resonant wavelengths depends on the polarization. Furthermore, it is worth noting that, in Fig. 2b and c the transmittance at the bandgap edges is not 100%, in contrast with the isotropic case. This is due to the fact that in the anisotropic case, besides the  $t_{xx}$  and  $t_{yy}$  components, the cross-polarization components  $t_{yx}$  and  $t_{xy}$  are nonzero, even for normal incidence.

The two degrees of freedom mentioned above confer properties to the structure that would not be possible if all the LC optical axes were parallel. In such case, there would be two resonances, due to the interaction of the two main polarizations with the ordinary and extraordinary refractive indices. However, there would not be the possibility of tuning simultaneously these two resonances by changing the optical axis angle in the  $xy$  plane, since these refractive indices are constant. With the independent variation of the LC optical axes at the mirrors and at the cavities this can be overcome. This tunability is possible because of the existence of the two LC optical axes directions. One of the LC optical axes fixes the main

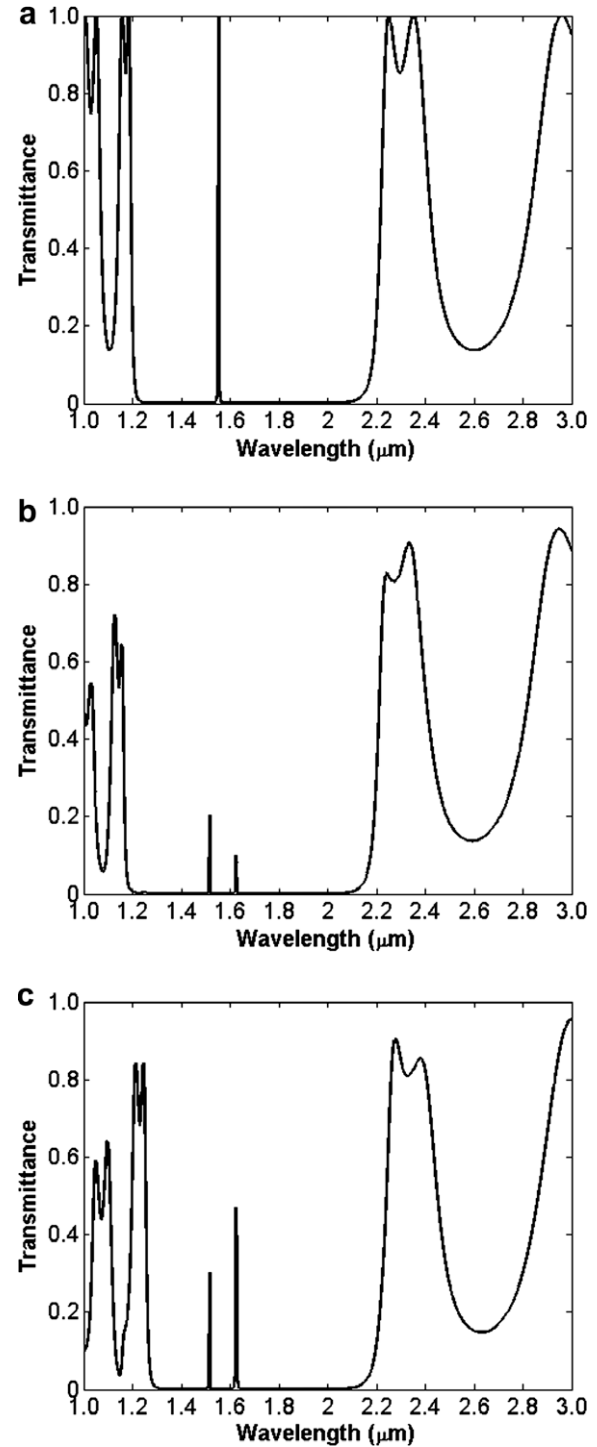


**Fig. 2.** Transmittance spectra for the structure  $[\text{HL}]^3\text{H}-\text{L}'-\text{H}[\text{LH}]^3$  (a) Isotropic state ( $n_{\text{olc}} = 1.585$ ,  $n_{\text{si}} = 3.4$ ). The structure is designed to have a resonance for  $\lambda = 1.55 \mu\text{m}$  in this state. (b)  $|t_{xx}|^2$  and (c)  $|t_{yy}|^2$  for the anisotropic state ( $\phi_M = 15^\circ$ ,  $\phi_C = 45^\circ$ ,  $n_{\text{olc}} = 1.522$ ,  $n_{\text{elc}} = 1.704$ ,  $n_{\text{si}} = 3.4$ ). The resonance present in the isotropic state splits in two,  $\lambda_1 = 1.516 \mu\text{m}$  and  $\lambda_2 = 1.625 \mu\text{m}$ .

polarization directions, while the second LC optical axis (with angle variable with respect to the first) is the one that actually influences the interaction of the incident light with the ordinary and extraordinary indexes.

The first property that we analyze is the tuning of the resonant wavelengths with the angles  $\phi_M$  and  $\phi_C$ . Since for normal incidence the election of the  $x$  and  $y$  axes (the main polarization directions) is free, this reduces the two degrees of freedom in the LC optical axes

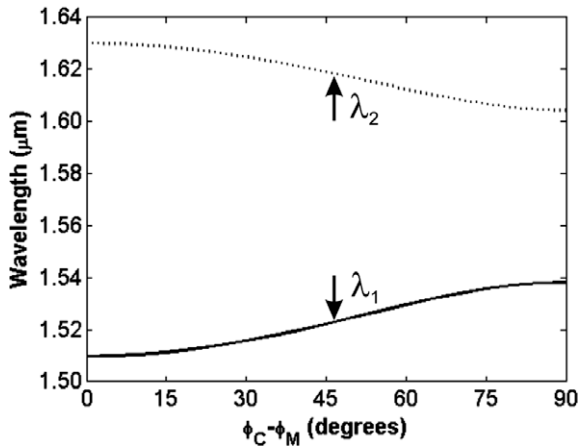


Fig. 3. Resonant wavelengths of the structure,  $\lambda_1$  (solid line) and  $\lambda_2$  (dotted line), versus the difference  $\phi_C - \phi_M$ .

to a single one consisting of the difference  $\phi_M - \phi_C$ . Fig. 3 shows the dependence of the two resonant wavelengths with this difference. As it can be seen, varying  $\phi_M - \phi_C$  from  $0^\circ$  to  $90^\circ$  the first resonance ( $\lambda_1$ ) can be tuned from  $1.510 \mu\text{m}$  to  $1.538 \mu\text{m}$  while the second ( $\lambda_2$ ) can be tuned simultaneously from  $1.630 \mu\text{m}$  to  $1.604 \mu\text{m}$ . Materials with higher anisotropy than E7 LC would enlarge this tuning range [27].

Fig. 4 shows the transmittance properties of the FP structure. The three graphs in Fig. 4 correspond to: (a)  $|t_{xx}|^2$ , (b)  $|t_{yy}|^2 = |t_{yx}|^2$  and (c)  $|t_{xy}|^2$ , calculated for the resonant wavelengths  $\lambda_1$  and  $\lambda_2$ . The calculations correspond to  $\phi_M = 0$  (mirror LC optical axis parallel to the y axis). The phase of  $t_{xx}$ ,  $t_{xy}$ ,  $t_{yx}$  and  $t_{yy}$  for  $\lambda_1$  is 0 for all  $\phi_C$ , while for  $\lambda_2$  the phase of  $t_{xx}$  and  $t_{yy}$  is 0 and the phase of  $t_{xy}$  and  $t_{yx}$  is  $\pi$ , also for all  $\phi_C$ . These values (the amplitudes of the transmission coefficient and their phases) describe completely the transmittance properties of the FP structure at the resonant wavelengths, in the form of its characteristic Jones matrix,  $J_{FP}(\phi_C; \phi_M = 0)$ . The transmittance for any combination of angles  $\phi_M$  and  $\phi_C$  can be deduced from these values with the Jones matrix formalism. This is accomplished using the adequate rotation matrixes. Thus, the Jones matrix of the FP system for any two angles  $\phi_C$  and  $\phi_M$  can be written as:

$$J_{FP}(\phi_C, \phi_M) = R^{-1}(\phi_M) J_{FP}(\phi_C; \phi_M = 0) R(\phi_M), \quad (9)$$

with  $R(\phi_M)$  the rotation matrix:

$$R(\phi_M) = \begin{pmatrix} \cos \phi_M & -\sin \phi_M \\ \sin \phi_M & \cos \phi_M \end{pmatrix}. \quad (10)$$

#### 4. Tunable two-channel optical equalizer based on a Fabry-Pérot structure infiltrated by liquid crystal

In order to obtain a working device, it is necessary to complement the FP structure presented in the previous section with other optical components that provide it with the desired functionality. By using a polarizer at the input of the device and an analyzer at the output, parallel to the input polarizer, we obtain a two-channel tunable equalizer. This is, a device that can change the resonant wavelengths and the relative transmittance between them as a function of the angles  $\phi_M$  and  $\phi_C$ . With the linear polarizers at the input and at the output of the FP structure oriented with the x direction, the transmittance of the device is proportional to the x-x component of the Jones matrix  $J_{FP}(\phi_C, \phi_M)$ ,  $t'_{xx}(\phi_C, \phi_M)$ . This component is related to the components of the  $J_{FP,0}(\phi_C, \phi_M = 0)$  through the expression:

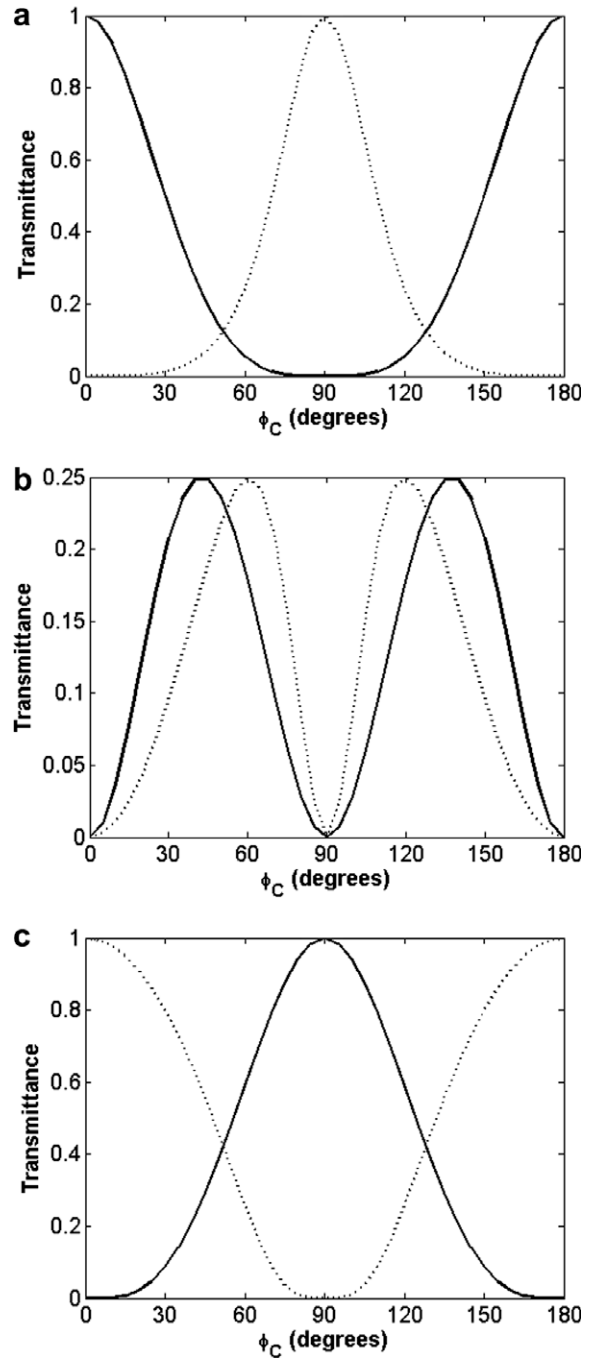
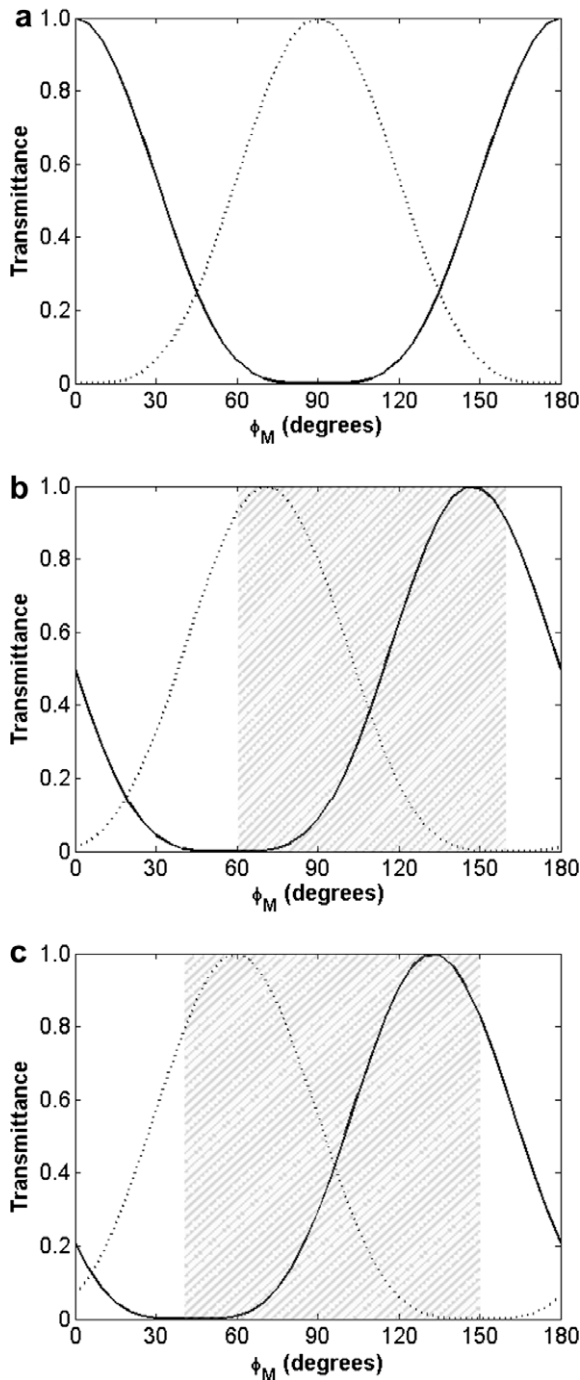


Fig. 4. Square modulus of the Jones matrix components of the FP structure at the resonant wavelengths  $\lambda_1$  (solid lines) and  $\lambda_2$  (dotted lines), versus the LC optical axis orientation at the cavity ( $\phi_M = 0^\circ$ ;  $\phi_C = [0^\circ - 180^\circ]$ ). (a)  $|t_{xx}|^2$ , (b)  $|t_{yy}|^2 = |t_{yx}|^2$  and (c)  $|t_{xy}|^2$ .

$$t'_{xx}(\phi_C, \phi_M) = t_{xx} \cos^2 \phi_M + t_{xy} \cos \phi_M \sin \phi_M + t_{yx} \cos \phi_M \sin \phi_M + t_{yy} \sin^2 \phi_M. \quad (11)$$

Fig. 5 shows the total transmittance of such a device when the LC optical axes are rotated between  $\phi_M = 0^\circ$  and  $\phi_M = 180^\circ$ , but with a fixed difference between their director angles. The three plots correspond to differences  $\phi_C - \phi_M = 0^\circ$  (a),  $\phi_C - \phi_M = 30^\circ$  (b) and  $\phi_C - \phi_M = 45^\circ$  (c). For  $\phi_C - \phi_M = 0^\circ$  the resonances are at  $\lambda_1 = 1.510 \mu\text{m}$  and  $\lambda_2 = 1.630 \mu\text{m}$ . The transmittance curves for the two resonant wavelengths are equal but shifted  $90^\circ$ . With this, the first resonance maximum ( $T = 100\%$ ) and the second resonance



**Fig. 5.** Transmittance at the resonant wavelengths  $\lambda_1$  (solid line) and  $\lambda_2$  (dotted line), of the optical two-channel equalizer for three angle differences. (a)  $\phi_C = \phi_M$ ,  $\lambda_1 = 1.510 \mu\text{m}$  and  $\lambda_2 = 1.630 \mu\text{m}$ . There is complete equalization: the maxima of one resonance correspond with the minima of the other ( $90^\circ$  relative shift between the transmittance curves) (b)  $\phi_C - \phi_M = 30^\circ$ ,  $\lambda_1 = 1.516 \mu\text{m}$  and  $\lambda_2 = 1.625 \mu\text{m}$ . The shift between the two transmittance curves is smaller than  $90^\circ$ . The equalization is not complete. The shaded region corresponds to the range of  $\phi_M$  with the better efficiency. (c)  $\phi_C - \phi_M = 45^\circ$ ,  $\lambda_1 = 1.522 \mu\text{m}$  and  $\lambda_2 = 1.619 \mu\text{m}$ . This case corresponds to the smallest relative shift between the transmittance curves.

minimum ( $T = 0\%$ ) appear for  $\phi_M = 0^\circ$  and  $\phi_M = 180^\circ$ , while the first resonance minimum and the second resonance maximum appear for  $\phi_M = 90^\circ$ . This means that in this configuration and for this pair of resonant wavelengths, there is *complete* equalization: one channel is completely suppressed while the other is completely transmitted. Another interesting feature in this configuration is that

for  $\phi_M = 45^\circ$  and  $\phi_M = 135^\circ$  the transmittance for the two resonant wavelengths intersect and this intersection level is the same for the two  $\phi_M$ .

For the case  $\phi_C - \phi_M = 30^\circ$  the resonant wavelengths are now  $\lambda_1 = 1.516 \mu\text{m}$  and  $\lambda_2 = 1.625 \mu\text{m}$ . The transmittances have shifted to the left in a different amount, thus the relative shift between the curves is smaller than in the previous case. This means that in this configuration the transmittance maxima of one resonance do not match with the minima of the other, and consequently the equalization is not complete. However, there are still configurations where one of the channels is completely blocked while the other is still transmitted with transmittance 85.47% (first resonance blocked,  $\phi_M = 60^\circ$ ) and 90.39% (second resonance blocked,  $\phi_M = 160^\circ$ ). Differently to the previous case, the intersection of the transmittance for the two resonant wavelengths is at different levels: 38.33% for  $\phi_M = 109^\circ$  and 14.66% for  $\phi_M = 19^\circ$ . Consequently, it is advisable to choose the adequate range of  $\phi_M$  (between  $\phi_M = 60^\circ$  and  $\phi_M = 160^\circ$ , indicated by the shaded region in the graph) to achieve a maximum efficiency of the device.

Finally, the case  $\phi_C - \phi_M = 45^\circ$  corresponds to the smallest shift between the transmittance spectra. The resonant wavelengths are now  $\lambda_1 = 1.522 \mu\text{m}$  and  $\lambda_2 = 1.619 \mu\text{m}$ . We include this case because it is the worst case: when one of the channels is blocked the transmittance of the other has the smallest transmittances, which are 78.58% (first resonance blocked,  $\phi_M = 40^\circ$ ) and 82.91% (second resonance blocked,  $\phi_M = 150^\circ$ ).

## 5. Conclusions

We have analyzed the transmittance properties of a tunable Fabry–Pérot structure composed of silicon and anisotropic materials, whose optical axes can be varied. The FP structure is composed of a cavity of anisotropic material surrounded by two mirrors, composed of successive layers of silicon and anisotropic materials. We have chosen E7 liquid crystal as anisotropic material because its optical axis can be electrically varied. In contrast with previous works, we have designed the structure so that the LC optical axes at the mirrors and at the cavity are always parallel to the layers and their direction in the mirrors or in the cavity can be varied independently.

Following the  $4 \times 4$  transfer matrix method, suited to multilayer structures with anisotropic materials, we are able to obtain the Jones matrix of the structure, and thus completely determine its transmission properties both in amplitude and in phase, and for the two main polarizations. Our results show that a tuning capability of 28 nm can be achieved as a function of the relative orientation between the LC optical axes. This range can be improved by substituting the E7 LC with an LC with a higher anisotropy.

The FP structure has been designed to have one resonance in the middle of the gap (at  $1.55 \mu\text{m}$ ) when the LC is in its isotropic state. When the LC is in its anisotropic state this resonance splits in two due to the interaction of the light with the ordinary and extraordinary indexes. The tuning of the resonant wavelengths and the associated transmittance is due to the existence of two independent LC optical axes within the mirrors and within the cavity.

On the basis of these results, we propose an optical two-channel equalizer that permits tuning the two resonances and their relative amplitude levels. This application is obtained by placing the FP structure in between two parallel linear polarizers. We have analyzed different relative orientations between the LC optical axes of this equalizer to determine its performance. Thus, for parallel optical axes we obtain complete equalization: one channel is completely suppressed ( $T = 0\%$ ) as the other is completely transmitted ( $T = 100\%$ ). In this case, we get the largest resonance split 120 nm. For other relative orientations of the LC optical axes, it is

apparent that the transmittances for each of the resonances shift with respect to each other and consequently complete equalization is not achieved. Nevertheless, complete blocking of one channel with respect to the other can be obtained. We have shown that the worst case corresponds to a difference in the optical axes orientation of  $45^\circ$ , in which the transmittance of the unblocked channel is as a minimum of 78.58% (first resonance blocked) and 82.91% (second resonance blocked). These figures show that the device can be useful with a good performance in a wide range of resonant frequencies.

### Acknowledgements

This work was supported by the Spanish Ministry of Science under Grants number TEC2006-06531 and HOPE CSD2007-00007 (Consolider-Ingenio 2010). J. Ferré-Borrull acknowledges the Ramon y Cajal fellowship from the Spanish Ministry of Science and Technology.

### References

- [1] S. John, Phys. Rev. Lett. 58 (1987) 2486.
- [2] E. Yablonovitch, Phys. Rev. Lett. 58 (1987) 2059.
- [3] O. Painter, R.K. Lee, A. Scherer, A. Yariv, J.D. O'Brien, P.D. Dapkus, I. Kim, Science 284 (1999) 1819.
- [4] R.D. Meade, K.D. Brommer, A.M. Rappe, J.D. Joannopoulos, Phys. Rev. B 44 (1991) 13772.
- [5] E. Centeno, D. Felbacq, Opt. Commun. 160 (1999) 57.
- [6] L.X. Chen, D. Kim, Opt. Commun. 218 (2003) 19.
- [7] H. Takeda, K. Yoshino, Opt. Commun. 219 (2003) 177.
- [8] I.S. Maksymov, L.F. Marsal, M.A. Ustyantsev, J. Pallarès, Opt. Commun. 248 (2005) 469.
- [9] K. Busch, S. John, Phys. Rev. Lett. 83 (1999) 967.
- [10] F. Cuesta-Soto, A. Martínez, J. García, F. Ramos, P. Sanchis, J. Blasco, J. Martí, Opt. Express 12 (2004) 161.
- [11] S. Weiss, H. Ouyang, J. Zhang, P. Fauchet, Opt. Express 13 (2005) 1090.
- [12] O.S. Heavens, Optical Properties of Thin Solid Films, Dover, 1965.
- [13] B.E. Perilloux, Thin-Film Design: Modulated Thickness and Other Stopband Design Methods, SPIE Press, 2002.
- [14] G. Alagappan, X.W. Sun, P. Shum, M.B. Yu, M.T. Doan, J. Opt. Soc. Am. B 23 (1) (2006) 159.
- [15] A. Mandatori, C. Sibilis, M. Centini, G. D'Aguanno, M. Bertolotti, M. Scalora, M. Bloemer, C.M. Bowden, J. Opt. Soc. Am. B 20 (3) (2003) 504.
- [16] C. Vandenbem, J.P. Vigneron, J.M. Vigoureux, J. Opt. Soc. Am. B 23 (11) (2006) 2366.
- [17] Y.K. Ha, Y.C. Yang, J.E. Kim, H.Y. Park, C.S. Kee, H. Lim, J.C. Lee, Appl. Phys. Lett. 79 (1) (2001) 15.
- [18] C.Y. Liu, L.W. Chen, Opt. Express 12 (2004) 2616.
- [19] K. Hirabayashi, H. Tsuda, T. Kurokawa, J. Lightwave Tech. 11 (12) (1993) 2033.
- [20] R. Ozaki, M. Ozaki, K. Yoshino, Elect. Commun. Jpn. 88 (4) (2005) 46.
- [21] D.C. Zografopoulos, E.E. Kriezis, B. Bellini, R. Beccherelli, Opt. Express 15 (4) (2007) 1832.
- [22] V.A. Tolmachev, T.S. Perova, S.A. Grudinkin, V.A. Melnikov, E.V. Astrova, Y.A. Zharova, Appl. Phys. Lett. 90 (2007) 011908.
- [23] J.M. Bennet, H.E. Bennet, in: W. Driscoll (Ed.), Handbook of Optics, McGraw-Hill, 1978.
- [24] A. Yariv, P. Yeh, Optical Waves in Crystals, Wiley, New York, 1984.
- [25] R.M.A. Azzam, N.M. Bashara, Ellipsometry and Polarized Light, North-Holland, 1989.
- [26] E. Hecht, Optics, Addison Wesley, 2002.
- [27] D. Demus, J.W. Goodby, G.W. Gray, Handbook of Liquid Crystals, vol. 2A, Wiley-VCH, 1998.